Polyubiquitin binding and cross-reactivity in the USP domain deubiquitinase USP21

Supplementary Material

Yu Ye[1], Masato Akutsu[1], Francisca Reyes-Turcu[2$], Radoslav I. Enchev[3#], Keith D. Wilkinson[2] and David Komander[1*]

[1]Medical Research Council Laboratory of Molecular Biology, Hills Road, Cambridge, UK

[2]Department of Biochemistry, Emory University School of Medicine, Atlanta, Georgia 303222, USA

[3]Section of Structural Biology, The Institute of Cancer Research, 237 Fulham Road, London, UK

$ Current address: Laboratory of Biochemistry and Molecular Biology, NCI, National Institutes of Health, Bethesda, Maryland 20892, USA

Current address: Institute of Biochemistry, ETH Hönggerberg HPM G10, CH-8093 Zürich

* Correspondence should be addressed to: David Komander, MRC Laboratory of Molecular Biology, Protein and Nucleic Acid Chemistry Division, Hills Road, Cambridge, CB2 0QH, UK. Email: dk@mrc-lmb.cam.ac.uk, Tel: +44 1223 402300, Fax: +44 1223 412178

Running title: Cross-reactivity in USP21

Experimental Procedures

Cloning

The human USP21 catalytic domain (residues 196-565) was PCR amplified from a pGFP vector (kind gift of Sylvie Urbe, Liverpool, UK) and cloned into the pOPINS vector (Berrow et al, 2007). This vector introduces an N-terminal 6xHis-SUMO tag in the USP21 construct. Expression of Ub, diUb and NEDD8 intein proteins was performed from pTYB2 constructs, and expression of ISG15 intein from the pTXB1 construct. In both vectors, the modifier is expressed as a fusion with intein and chitin binding domains. The diUb contains a non-cleavable linker between the Ub moieties with sequence Gly75-His76 instead of Gly75-Gly76 (Drag et al, 2008). The ISG15 probes contained a point mutation (C78S) required for stability and high-level expression of ISG15 (Narasimhan et al, 2005). All point mutants were generated using site-directed mutagenesis with PAGE-purified forward and reverse primers. PCR reactions were carried out by Cod polymerase (Merck BioSciences) according to manufacturer protocols, followed by 1 h restriction digest using *Dpn*I and subsequent transformation into Mach1 cells (Invitrogen).

USP21 protein expression

pOPINS-USP21 (196-565) was transformed into *E.coli* Rosetta 2 pLysS (Novagen) and grown to OD 1.0 followed by 1 mM IPTG overnight induction at 20°C. Cells were lysed by sonication in buffer A (50 mM Tris, 300 mM NaCl, 10 mM imidazole, pH 7.4), the lysate was cleared by centrifugation (44000 x g for 30 min, 4°C) and subjected to a self-packed TALON (Clontech) column on an ÄKTA Explorer HPLC system. The bound protein was eluted with buffer B (50 mM Tris, 300 mM NaCl, 200 mM imidazole, pH 7.4) and cleaved with SENP1 to remove the His-SUMO tag. Subsequently, the protein was dialyzed against the gel filtration buffer (25 mM Tris, 200 mM NaCl, 5 mM DTT, pH 7.4) before a final gel filtration step. The final protein was 98% pure

judged by SDS-PAGE and the yield is 10 mg of pure protein per litre cell culture.

Suicide probe expression and purification

pTYB2 vectors were transformed into Rosetta2 pLacI cells (Novagen), and cells were grown to OD 1.0, followed by induction with 0.5 mM IPTG and protein expression at 20°C overnight. Lysis buffer consisted of 50 mM HEPES, 100 mM NaCl, 100 mM sodium acetate [pH 6.5] and cell lysates were prepared and cleared as described above. Cleared lysate was filtered and incubated with chitin beads at room temperature for 3 h. The beads were washed with 0.5x Lysis buffer and 0.5x Lysis buffer containing 550 mM NaCl. Intein cleavage was performed overnight at 4°C with 200 mM sodium 2-sulfanylethanesulfonate (Mesna). The eluted fractions of free Ub/Ubl thiol ester were concentrated to 2 mg/ml and buffer exchanged into 25 mM HEPES, 50 mM NaCl, 50 mM sodium acetate [pH 6.5].

USP21 complex reaction with Ub/Ubl suicide probes

Generation of suicide inhibitors was performed according to published protocols (Borodovsky et al, 2002; Love et al, 2007). 250 μl of 2-5 mg/ml Ub/Ubl thiol ester was used to dissolve 12 mg, 21 mg or 22 mg of 2-bromoethylamine hydrobromide (C2Br), 2-chloroethylamine hydrochloride (C2Cl) and 3-bromopropyllamine hydrobromide (C3Br), respectively. 50 μl of 2 M NaOH was used to activate the covalent bond formation and the reactions were subsequently stopped after 1 h using 50 μl 2 M HCl. The probes were dialyzed against 50 mM NaCl, 25 mM Tris [pH 7.0] for 1 h at room temperature.

For complex formation, deubiquitinases were diluted to 0.5-2 mg/ml and 20 μl was allowed to react with 50 μl of probe (1.5-2 mg/ml) at room temperature. Samples of 20 μl were taken at indicated time points and the reaction was stopped with 10 μl of 4x LDS loading buffer (Invitrogen). 10 μl of this sample

were resolved by SDS-PAGE and stained by InstantBlue Coomassie stain (Expedeon).

Protein complex generation for crystallography

DiUb-acetal was converted to diUb-aldehyde by adding 15% of total volume of 2 M HCl for 3 h at room temperature. The reaction was stopped by adding an equivalent volume of 2 M NaOH (Hershko & Rose, 1987). Complex formation with USP21 was performed in gel filtration buffer for 1 h. The resulting USP21•diUb complex was purified by gel filtration to remove unreacted proteins.

Crystallisation, data collection and refinement

Crystallisation screening commenced at 6.7 mg/ml final complex concentration and thin needle crystals formed overnight from 15% PEG8000, 0.2 M NH_4SO_4. Crystals were soaked in mother liquor containing 25% PEG400 prior to flash freezing in a nitrogen cryo-stream. Diffraction data were collected at ESRF beamline ID23-2 (**Supplementary Table 1**). The diffraction data was processed using iMosflm (Leslie, 2006) and the CCP4 software suite. The structure was solved by molecular replacement, using USP2 (pdb-id 2hd5, (Renatus et al, 2006)) and monoUb (pdb-id 1ubq (Vijay-Kumar et al, 1987)) as search models in Phaser (McCoy et al, 2005). Subsequent rounds of model building and refinement were carried out in Coot (Emsley & Cowtan, 2004) and Refmac (Murshudov et al, 1997). Prediction of complex surface interaction was preformed by the Pisa server (http://www.ebi.ac.uk/msd-srv/prot_int/pistart.html).

Deubiquitination assays

Qualitative deubiquitinase assays against different Ub chain linkages were carried out according to (Komander et al, 2009). In essence, deubiquitinases

were diluted to 0.2 μg/μl in the reaction buffer (150 mM NaCl, 25 mM Tris, 10 mM DTT, pH 7.4). At indicated time points after reaction initiation, 6 μl reaction aliquots were taken and the reaction was stopped by adding 4 μl of 4x LDS loading buffer (Invitrogen). 5 μl samples were run on 4-12% NuPage gel in MES buffer (Invitrogen), followed by silver staining (Bio-Rad) or staining with SYBRO Ruby (BioRad). Gels were scanned on a Typhoon Imager, and gel bands were quantified using ImageQuant TL software.

Expression and Purification of FlAsH-tagged linear di- and triUb

MonoUb, and linear di- and triUb in which the C-terminal five residues were replaced with a WCCPGCC FlAsH-tag sequence, were generated in the pRS vector and expressed in B834 (DE3) pLysS cells (Invitrogen). Ub chains were purified according to (Virdee et al, 2010). The concentration of each Ub chain was determined by NanoDrop due to the presence of the additional Trp residue. Labelling with Lumio Green (Invitrogen) was performed as per manufacturers manual and the concentration of the labelled (poly)Ub was determined by Nanodrop using the wavelength of the fluorophore.

Fluorescence measurements

Ub- and ISG15-amidomethyl coumarin (AMC) probes were purchased from Boston Biochem and NEDD8-AMC was purchased from BioMol. Fluorescence measurements to detect released AMC were performed on a Vary Eclipse fluorimeter with excitation and emission wavelengths at 340 nm and 440 nm, respectively, in Quartz cuvettes (Hellma, 105.250-QS). The concentration of enzymes were measured in the linear range of NanoDrop sensitivity, diluted to 50 μM and then stepwise diluted to a concentration of 2 nM for Ub-AMC measurements, and 20 nM for ISG15-AMC measurements. The final concentration for UCH-L3 was 50 nM in all assays. The final enzyme stock was activated with 5 mM DTT for 10 min before measurement. Reactions were performed in 150 μl or 120 μl final volume, in Reaction buffer

(200 mM NaCl, 50 mM Tris, 100 μg/ml BSA, 5 mM DTT, pH 7.4). A baseline of AMC fluorescence was acquired by measuring fluorescent probes in Reaction buffer for 60-120 s prior to adding 10x concentrated enzyme to the reaction. The reactions were followed for 900 s in total, and all measurements were performed in triplicate.

In order to determine Michaelis-Menten kinetics, duplicate reactions were performed at varying substrate concentration in 20 µl reaction volume, and fluorescence intensity was followed in 384 well format employing a Pherastar FS plate reader with excitation and emission wavelengths at 350 nm and 450 nm. A standard curve was determined using free AMC at known concentrations. We observed that USP21 was inhibited by low concentrations (2% v/v) of glycerol present in the ISG15-AMC preparation, and corrected for this buffer effect by serial dilution of substrate until the effect was negligible.

The PheraStar FS was also used in the binding assay based on the fluorescence anisotropy of linear Ub chains. Fluorescently labelled linear ubiquitin chains were diluted to 80 nM in FlAsH buffer (50 mM Tris, 50 mM NaCl, 0.1% β-mercaptoethanol, pH 7.6). Wild-type or mutant USP21i were serially diluted in FlAsH buffer to the indicated concentration range (**Fig. 3F, G**). 10 µl of the fluorescent Ub chain was mixed with equal volume of USP21i at different concentrations and incubated in room temperature for 1 h before measurement. Fluorescence anisotropy was measured in 384 well format employing a Pherastar FS plate reader, using a fluorescence polarisation module with excitation and emission wavelengths at 485 nm and 520 nm respectively. A control was used for either linear di- or triUb molecules where 10 µl of FlAsH buffer was added instead. This control was also used for the normalization of anisotropy reading. All binding assays were performed in triplicate.

Generation of ISGylated substrates and deISGylation assay

Protein ISGylation was induced in HeLa cells with IFN-β according to (Durfee et al, 2010). 1000 units/ml of IFN-β (Betaseron) was used and the cells were

incubated for 24 h at 37°C, followed by lysis in 500 µl of EMBO lysis buffer (150 mM NaCl, 30mM Tris HCl pH 7.4, 2 mM EDTA 10 glycerol, 1mM sodium orthovanadate, 1 mM NaF, 0.5 % NP40) using standard protocols. The lysate was further cleared in a benchtop centrifuge at 13200 rpm for 10 min at 4°C. 15 µl of the supernatant was used in incubation with wild-type or mutant USP21 at 1 mg/ml for 1 h at 37°C. The reaction was stopped with 5 µl of LDS buffer. 7 µl of the samples were subsequently loaded onto a 4-12% SDS-PAGE gel, with the same amount of USP21 only and HeLa supernatant as control and 2 µg of ISG15 as the positive control. Protein bands were transferred to PVDF paper and ISGylated proteins were visualized by western blot using an anti-ISG15 antibody (H-150, SantaCruz). After luminescence detection with SuperSignal ECL reagent (Fisher), the PVDF membrane was stained with Ponceau S solution (Sigma).

NEDD8~Cul1 deNeddylation assay

Neddylated cullin1 (NEDD8~Cul1) was generated according to published protocol (Enchev et al, 2010). For the deNeddylation assay, 4 µl of NEDD8~Cul1 at 0.5 mg/ml was mixed together with 3 µl of 10× DUB buffer (150 mM NaCl, 25 mM Tris, 10 mM DTT, pH 7.4) and 13 µl of H_2O. To initiate the reaction, 10 µl of either USP21 or COP9 signalosome (CSN) at 0.02 mg/ml was added to the NEDD8~Cul1. At each indicated timepoint, 6 µl reaction sample was taken and inactivated with 5 µl of LDS. 5 µl of each timepoint sample was consequently loaded onto a 4-12% SDS-PAGE gel together with 10× NEDD8~Cul1 as control.

Supplementary References

Berrow NS, Alderton D, Sainsbury S, Nettleship J, Assenberg R, Rahman N, Stuart DI, Owens RJ (2007) A versatile ligation-independent cloning method suitable for high-throughput expression screening applications. *Nucleic Acids Res* **35**(6)**:** e45

Borodovsky A, Ovaa H, Kolli N, Gan-Erdene T, Wilkinson KD, Ploegh HL, Kessler BM (2002) Chemistry-based functional proteomics reveals novel members of the deubiquitinating enzyme family. *Chem Biol* **9**(10)**:** 1149-1159

Drag M, Mikolajczyk J, Bekes M, Reyes-Turcu FE, Ellman JA, Wilkinson KD, Salvesen GS (2008) Positional-scanning fluorigenic substrate libraries reveal unexpected specificity determinants of DUBs (deubiquitinating enzymes). *Biochem J* **415**(3)**:** 367-375

Durfee LA, Lyon N, Seo K, Huibregtse JM (2010) The ISG15 conjugation system broadly targets newly synthesized proteins: implications for the antiviral function of ISG15. *Mol Cell* **38**(5)**:** 722-732

Emsley P, Cowtan K (2004) Coot: model-building tools for molecular graphics. *Acta Crystallogr D Biol Crystallogr* **60**(Pt 12 Pt 1)**:** 2126-2132

Enchev RI, Schreiber A, Beuron F, Morris EP (2010) Structural insights into the COP9 signalosome and its common architecture with the 26S proteasome lid and eIF3. *Structure* **18**(4)**:** 518-527

Frias-Staheli N, Giannakopoulos NV, Kikkert M, Taylor SL, Bridgen A, Paragas J, Richt JA, Rowland RR, Schmaljohn CS, Lenschow DJ, Snijder EJ, García-Sastre A, Virgin HW (2007) Ovarian tumor domain-containing viral proteases evade ubiquitin- and ISG15-dependent innate immune responses. *Cell Host Microbe* **2**(6)**:** 404-416

Hershko A, Rose IA (1987) Ubiquitin-aldehyde: a general inhibitor of ubiquitin-recycling processes. *Proc Natl Acad Sci U S A* **84**(7)**:** 1829-1833

Komander D, Reyes-Turcu F, Licchesi JD, Odenwaelder P, Wilkinson KD, Barford D (2009) Molecular discrimination of structurally equivalent Lys 63-linked and linear polyubiquitin chains. *EMBO Rep* **10**(5)**:** 466-473

Leslie AG (2006) The integration of macromolecular diffraction data. *Acta Crystallogr D Biol Crystallogr* **62**(Pt 1)**:** 48-57

Love KR, Catic A, Schlieker C, Ploegh HL (2007) Mechanisms, biology and inhibitors of deubiquitinating enzymes. *Nat Chem Biol* **3**(11)**:** 697-705

McCoy AJ, Grosse-Kunstleve RW, Storoni LC, Read RJ (2005) Likelihood-enhanced fast translation functions. *Acta Crystallogr D Biol Crystallogr* **61**(Pt 4)**:** 458-464

Misaghi S, Galardy PJ, Meester WJN, Ovaa H, Ploegh HL, Gaudet R (2005) Structure of the ubiquitin hydrolase UCH-L3 complexed with a suicide substrate. *J Biol Chem* **280**(2)**:** 1512-1520

Murshudov GN, Vagin AA, Dodson EJ (1997) Refinement of macromolecular structures by the maximum- likelihood method. *Acta Crystallographica Section D-Biological Crystallography* **53:** 240-255

Narasimhan J, Wang M, Fu Z, Klein JM, Haas AL, Kim J-JP (2005) Crystal structure of the interferon-induced ubiquitin-like protein ISG15. *J Biol Chem* **280**(29)**:** 27356-27365

Renatus M, Parrado SG, D'Arcy A, Eidhoff U, Gerhartz B, Hassiepen U, Pierrat B, Riedl R, Vinzenz D, Worpenberg S, Kroemer M (2006) Structural basis of ubiquitin recognition by the deubiquitinating protease USP2. *Structure* **14**(8)**:** 1293-1302

Vijay-Kumar S, Bugg CE, Cook WJ (1987) Structure of ubiquitin refined at 1.8 A resolution. *J Mol Biol* **194**(3)**:** 531-544

Virdee S, Ye Y, Nguyen DP, Komander D, Chin JW (2010) Engineered diubiquitin synthesis reveals Lys29-isopeptide specificity of an OTU deubiquitinase. *Nat Chem Biol* **6**(10)**:** 750-757

Wilkinson KD, Gan-Erdene T, Kolli N (2005) Derivitization of the C-terminus of ubiquitin and ubiquitin-like proteins using intein chemistry: methods and uses. *Meth Enzymol* **399:** 37-51

Supplementary Table 1

Data collection and refinement statistics. Values between brackets are for the highest resolution shell.

	USP21~diUb
Data collection statistics	
Beamline	ID23-2
Wavelength (Å)	1.0000
Space Group	$P2_1$
Unit Cell (Å)	a = 57.87, b = 102.20, c = 86.80, β = 99.82
Resolution (Å)	49.80 - 2.70 (2.85-2.70)
Observed reflections	71900 (10041)
Unique reflections	24840 (3397)
Redundancy	2.9 (3.0)
Completeness (%)	91.1 (86.2)
R_{merge}	0.120 (0.474)
$<I/\sigma I>$	8.8 (2.4)
Refinement statistics	
Reflections in test set	1267
R_{cryst}	0.216
R_{free}	0.276
Number of groups	
Protein residues	944
Solvent atoms	86
Wilson B ($Å^2$)	42.3
$<B>$ protein ($Å^2$)	21.5
$<B>$ solvent ($Å^2$)	31.7
RMSD from ideal geometry	
Bond length (Å)	0.007
Bond angles (°)	1.035

Supplementary Figure legends

Supplementary Figure 1: NEDD8 control experiments.

A) The intein system was utilised to generate Ub and NEDD8 suicide inhibitors (Wilkinson et al, 2005). A non-cleavable linear diUb-thioester (Drag et al, 2008) and a NEDD8-thioester were converted to suicide inhibitors by modification with 2-bromoethylamine hydrobromide (C2Br), 2-chloroethylamine hydrochloride (C2Cl) and 3-bromopropyllamine hydrobromide (C3Br) (Borodovsky et al, 2002). These suicide inhibitors attach covalently to the USP domain catalytic Cys residue, resulting in an increase in molecular weight of the protein by the mass of the modifier (17kDa and ~8kDa for diUb and NEDD8, respectively), resolvable by SDS-PAGE. NEDD8 and diUb suicide probes were incubated with purified USP21 at room temperature for 1 h. The coomassie-stained gel shows the band-shift for USP21 with the three diUb-based suicide inhibitors, while NEDD8 suicide probes do not result in a band-shift. Equivalent results were obtained for longer incubation periods (24 h, data not shown). B) Ub- and NEDD8-AMC substrates are cleaved readily by UCH-L3, as has been reported previously (Misaghi et al, 2005). The assay was performed as in **Fig. 1A** in the main text. C) Cullin deneddylation assay. NEDD8-modified Cul1 was prepared according to (Enchev et al, 2010). Deneddylation reactions were performed according to the protocol for deubiquitination reactions. While USP21 incubation does not result in any change of Cul1 deneddylation, the COP9 signalosome (CSN) hydrolyses NEDD8 from Cul1 (positive control).

Supplementary Figure 2: Quantification of deubiquitinase specificity.

A) Time course analysis of wild-type USP21 against differently linked Ub tetramers resolved on SDS-PAGE, visualised with SYBR orange protein stain (BioRad). USP21 enzyme concentration was reduced in order to see reaction intermediates. B) The gel was subsequently scanned using a TYPHOON scanner, and individual bands quantified using rubberband analysis. The

graphs represent quantification of bands corresponding to Ub tetramers, trimers, dimers and monomers as % corresponding to the input material.

Supplementary Figure 3: Structural sequence alignment

Sequence alignment of USP21 from various species and human USP2, with secondary structure elements indicated and labelled, corresponding to USP21 (top) and USP2 (bottom). Numbering refers to human USP21. A red background indicates invariant residues. Catalytic triad residues are boxed in yellow, Zn-coordinating residues in blue, and residues in the S2 binding site in purple. Grey boxes in the human USP21 sequence indicate disordered regions.

Supplementary Figure 4: Crystal packing and crystal contacts in USP21~diUb crystals.

A) Content of the asymmetric unit, showing the different relative positions of the distal Ub moiety. In complex A (bottom), the distal moiety is bound at the S2 Ub binding site. In complex B (top) the distal moiety is not contacted by USP21, resulting in high mobility and weak electron density. B) 2|Fo|-|Fc| electron density for the distal Ub moieties in both complexes, contoured at 1 σ. The disordered moiety in complex B was modelled with a polyAla backbone, while in complex A, side chains were well defined.

Supplementary Figure 5: Structural implications of Ub binding to USP21

A) USP21 and the S1 Ub are shown in cartoon representation, and Lys residues and N-terminus of Ub are indicated in stick representation. The S2-binding site at the back of the Fingers domain is labelled. The Ub molecule bound to the S1 site of the USP domain is spatially restrained because the extensive interactions restrict flexibility and determine the Ub orientation. This fixes the relative position of the S1 Ub Lys side chains, which in case of endo-
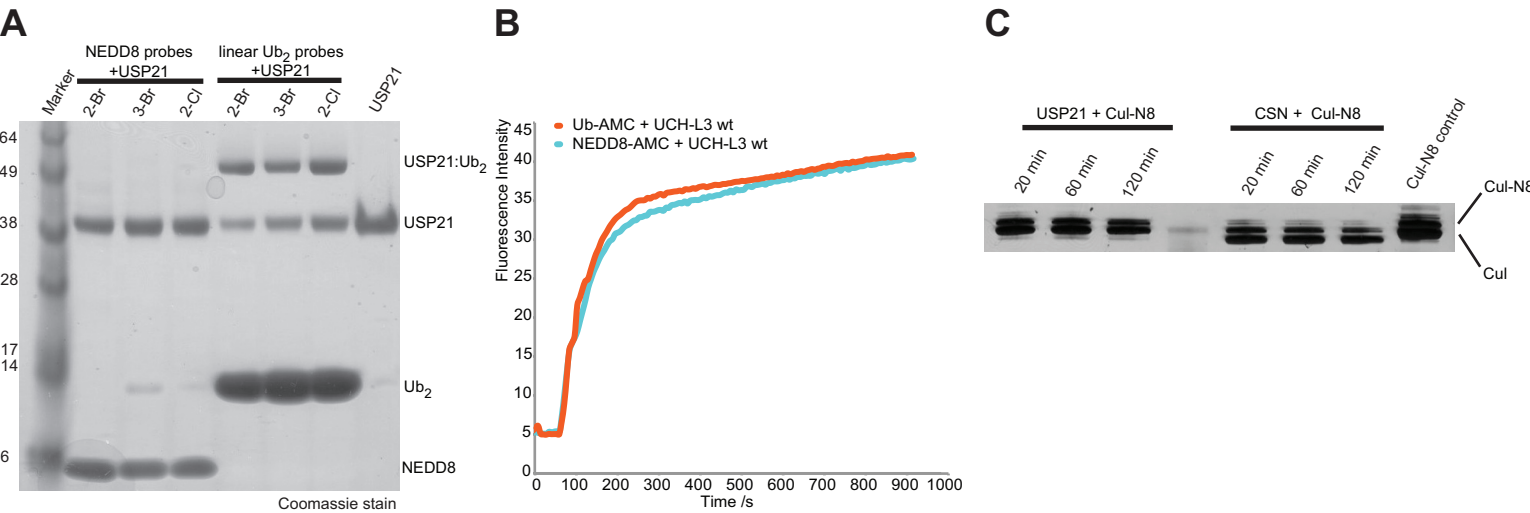
activity would carry further Ub moieties. For instance, Lys6 of the S1 Ub is buried at the USP domain interface, and extension of a Ub chain at this residue is unlikely and USP domains may cleave K6-linked chains with an *exo*-activity from the distal end. The remaining Lys side chains are exposed, and extended K63- and possibly for K29- and K33-linked Ub chains may benefit from additional binding interfaces at the S2 site. B) Superposition of the C-terminal Ubl-fold of ISG15 (magenta) onto Ub (yellow) in the S1 site of USP21 (grey), in two orientations. Since ISG15 hydrolysis is affected in S2 binding site mutants, ISG15 undergoes a conformational change to adopt a structure resembling linear diUb (indicated by arrows).

Supplementary Figure 6: USP21 binding to Ub-FlAsH

MonoUb in which the C-terminal five residues (RLRGG) were replaced with a Trp-FlAsH-sequence (WCCPGCC) does not bind to USP21 in fluorescence anisotropy studies. Error bars represent standard deviation from mean.

Supplementary Figure 7: ISG15 suicide probe assays

ISG15 and mutant ISG15 suicide probes (ISG15-C2Cl, and ISG15^{R153A}-C2Cl) were generated and tested against USP21^{wt} and USP21^{E304A}. Arg153 in ISG15 corresponds to Arg72 in Ub. Only wild-type proteins (i.e. USP21^{wt} and ISG15-C2Cl) resulted in covalent modification, and neither the USP21^{E304A} mutant, nor a mutant probe ISG15^{R153A}-C2Cl), generated a covalent modifier complex. Modification of USP21 with ISG15 suicide probes was not quantitative, suggesting lower reactivity towards this probe, consistent with lower activity of USP21 against ISG15-AMC. UCH-L3 is not modified by ISG15 probes, and hence as a positive control, a recently described viral OTU domain of Crimean Congo hemorrhagic fever virus (CCHFV, (Frias-Staheli et al, 2007)) with cross-reactivity against Ub and ISG15 was utilised. This enzyme was modified quantitatively with ISG15-C2Cl and to a lesser extent with ISG15^{R153A}-C2Cl. All ISG15 probes comprised the stabilising C78S mutation, indicated by ISG15* (Narasimhan et al, 2005).
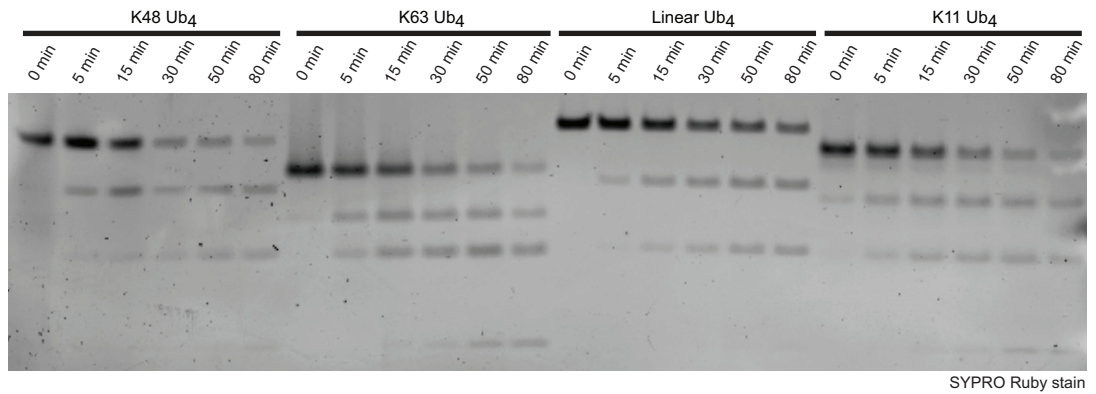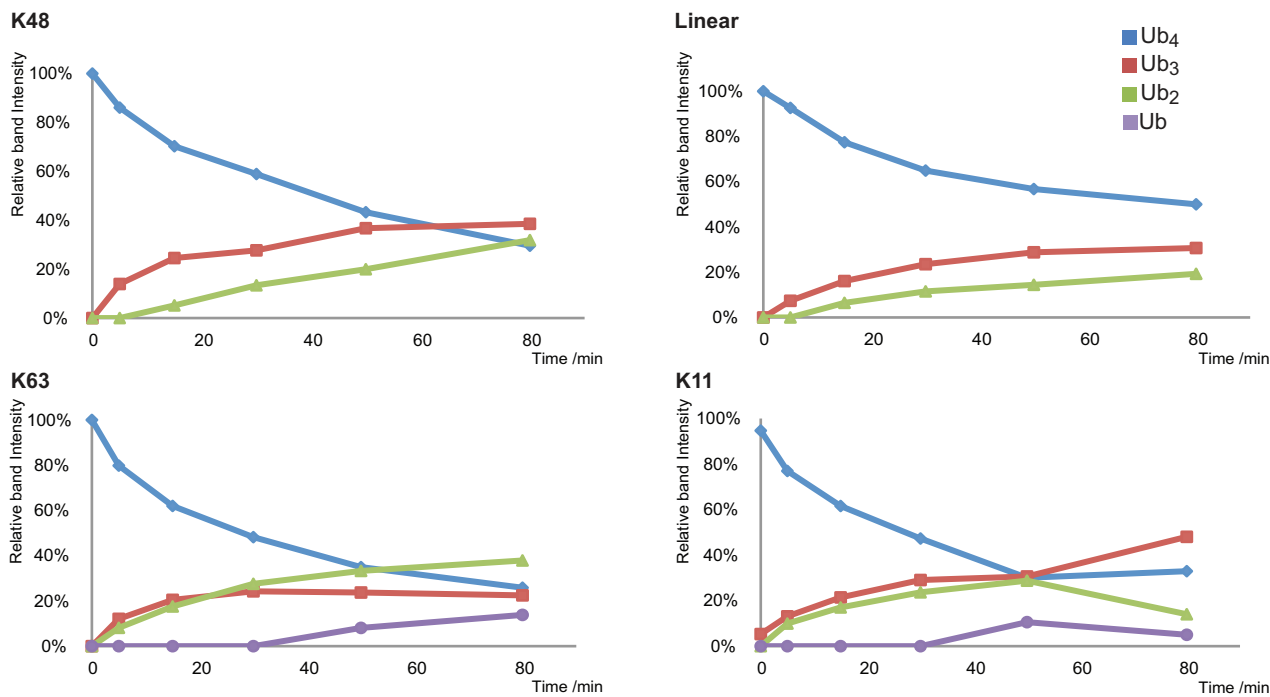
Supplementary Figure 1: NEDD8 control experiments.

A) The intein system was utilised to generate Ub and NEDD8 suicide inhibitors (Wilkinson et al, 2005). A non-cleavable linear diUb-thioester (Drag et al, 2008) and a NEDD8-thioester were converted to suicide inhibitors by modification with 2-bromoethylamine hydrobromide (C2Br), 2-chloroethylamine hydrochloride (C2Cl) and 3-bromopropyllamine hydrobromide (C3Br) (Borodovsky et al, 2002). These suicide inhibitors attach covalently to the USP domain catalytic Cys residue, resulting in an increase in molecular weight of the protein by the mass of the modifier (17kDa and ~8kDa for diUb and NEDD8, respectively), resolvable by SDS-PAGE. NEDD8 and diUb suicide probes were incubated with purified USP21 at room temperature for 1 h. The coomassie-stained gel shows the band-shift for USP21 with the three diUb-based suicide inhibitors, while NEDD8 suicide probes do not result in a band-shift. Equivalent results were obtained for longer incubation periods (24 h, data not shown).
B) Ub- and NEDD8-AMC substrates are cleaved readily by UCH-L3, as has been reported previously (Misaghi et al, 2005). The assay was performed as in Fig. 1A in the main text.
C) Cullin deneddylation assay. NEDD8-modified Cul1 was prepared according to (Enchev et al, 2010). Deneddylation reactions were performed according to the protocol for deubiquitination reactions. While USP21 incubation does not result in any change of Cul1 deneddylation, the COP9 signalosome (CSN) hydrolyses NEDD8 from Cul1 (positive control).
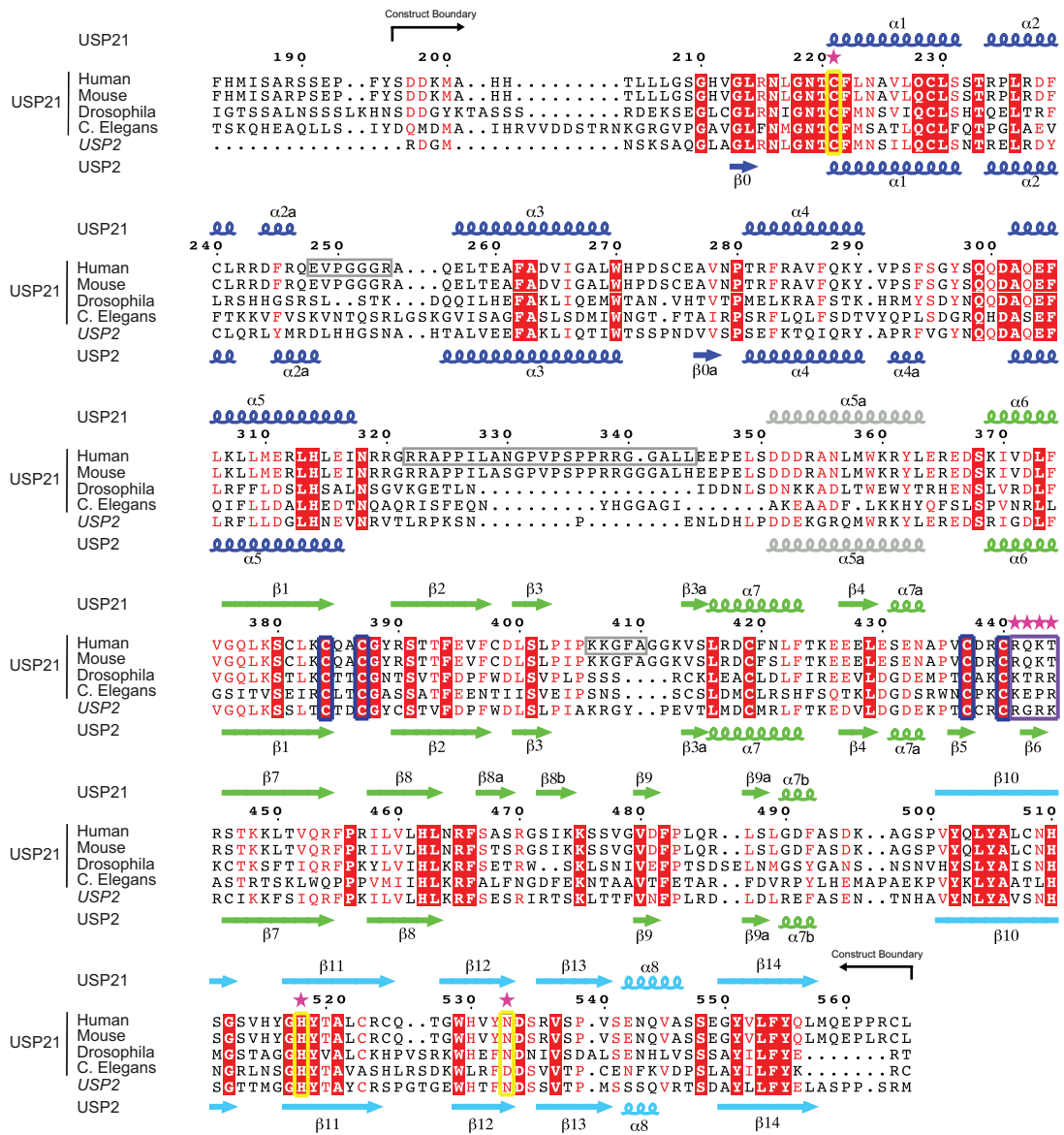
A

B

Supplementary Figure 2: Quantification of deubiquitinase specificity.

A) Time course analysis of wild-type USP21 against differently linked Ub tetramers resolved on SDS-PAGE, visualised with SYBR orange protein stain (BioRad). USP21 enzyme concentration was reduced in order to see reaction intermediates. B) The gel was subsequently scanned using a TYPHOON scanner, and individual bands quantified using rubberband analysis. The graphs represent quantification of bands corresponding to Ub tetramers, trimers, dimers and monomers as % corresponding to the input material.

Supplementary Figure 3: Structural sequence alignment

Sequence alignment of USP21 from various species and human USP2, with secondary structure elements indicated and labelled, corresponding to USP21 (top) and USP2 (bottom). Numbering refers to human USP21. A red background indicates invariant residues. Catalytic triad residues are boxed in yellow, Zn-coordinating residues in blue, and residues in the S2 binding site in purple. Grey boxes in the human USP21 sequence indicate disordered regions.
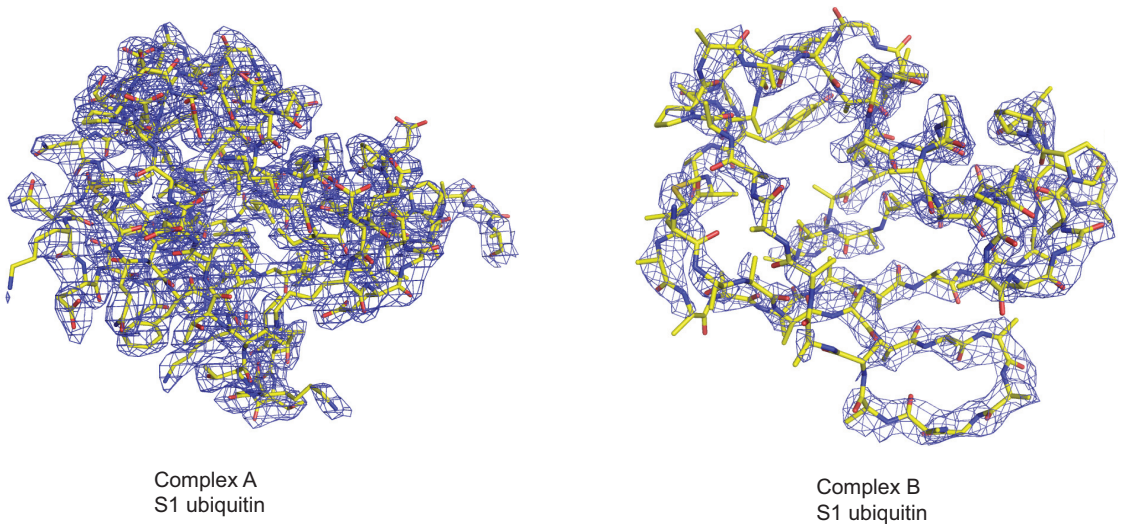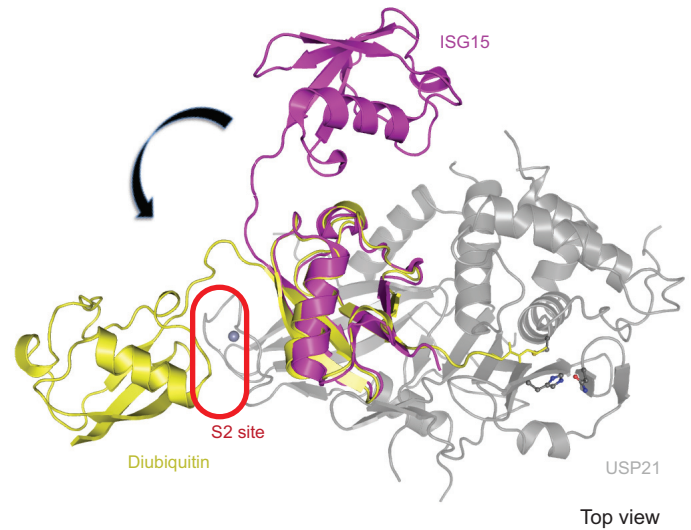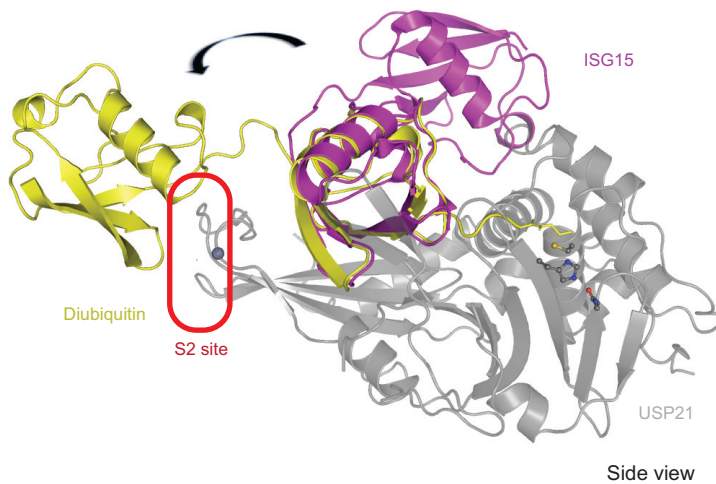
A Content of asymmetric unit

B Electron density of distal ubiquitin molecules

Supplementary Figure 4: Crystal packing and crystal contacts in USP21~diUb crystals.
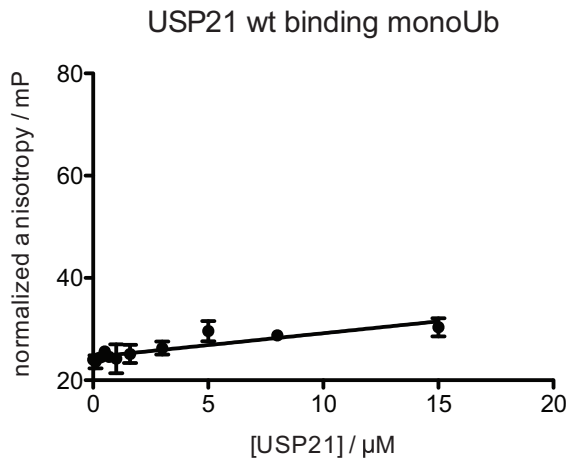
A) Content of the asymmetric unit, showing the different relative positions of the distal Ub moiety. In complex A (bottom), the distal moiety is bound at the S2 Ub binding site. In complex B (top) the distal moiety is not contacted by USP21, resulting in high mobility and weak electron density. B) 2|Fo|-|Fc| electron density for the distal Ub moieties in both complexes, contoured at 1 σ. The disordered moiety in complex B was modelled with a polyAla backbone, while in complex A, side chains were well defined.

A Lys positions on S1 ubiquitin

Side view

Top view
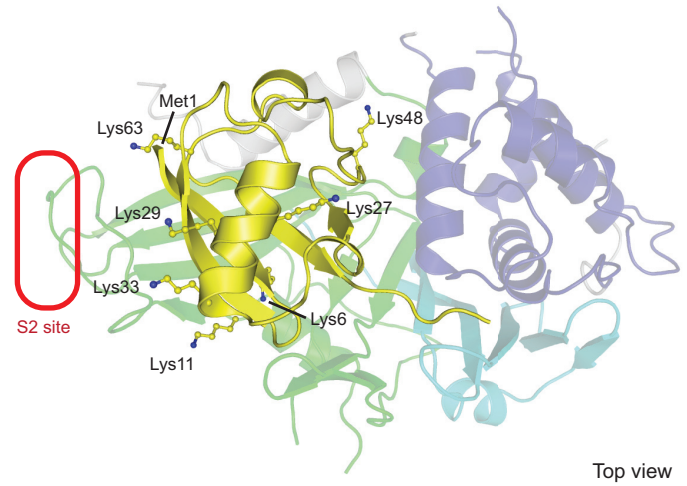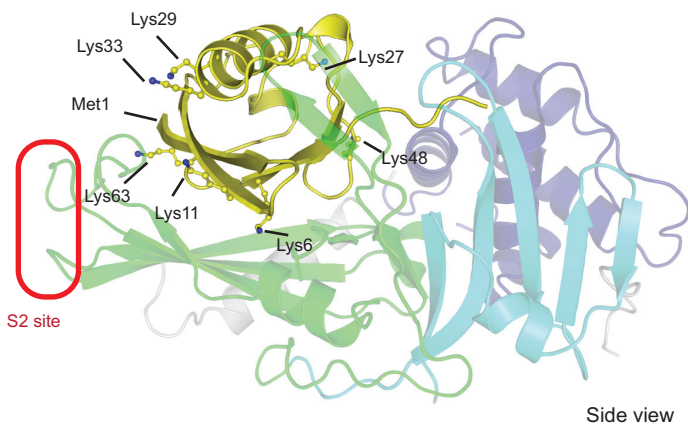
B ISG15 conformational change

Side view

Top view

Supplementary Figure 5: Structural implications of Ub binding to USP21

A) USP21 and the S1 Ub are shown in cartoon representation, and Lys residues and N-terminus of Ub are indicated in stick representation. The S2-binding site at the back of the Fingers domain is labelled. The Ub molecule bound to the S1 site of the USP domain is spatially restrained because the extensive interactions restrict flexibility and determine the Ub orientation. This fixes the relative position of the S1 Ub Lys side chains, which in case of endo-activity would carry further Ub moieties. For instance, Lys6 of the S1 Ub is buried at the USP domain interface, and extension of a Ub chain at this residue is unlikely and USP domains may cleave K6-linked chains with an exo-activity from the distal end. The remaining Lys side chains are exposed, and extended K63- and possibly for K29- and K33-linked Ub chains may benefit from additional binding interfaces at the S2 site. B) Superposition of the C-terminal Ubl-fold of ISG15 (magenta) onto Ub (yellow) in the S1 site of USP21 (grey), in two orientations. Since ISG15 hydrolysis is affected in S2 binding site mutants, ISG15 undergoes a conformational change to adopt a structure resembling linear diUb (indicated by arrows).
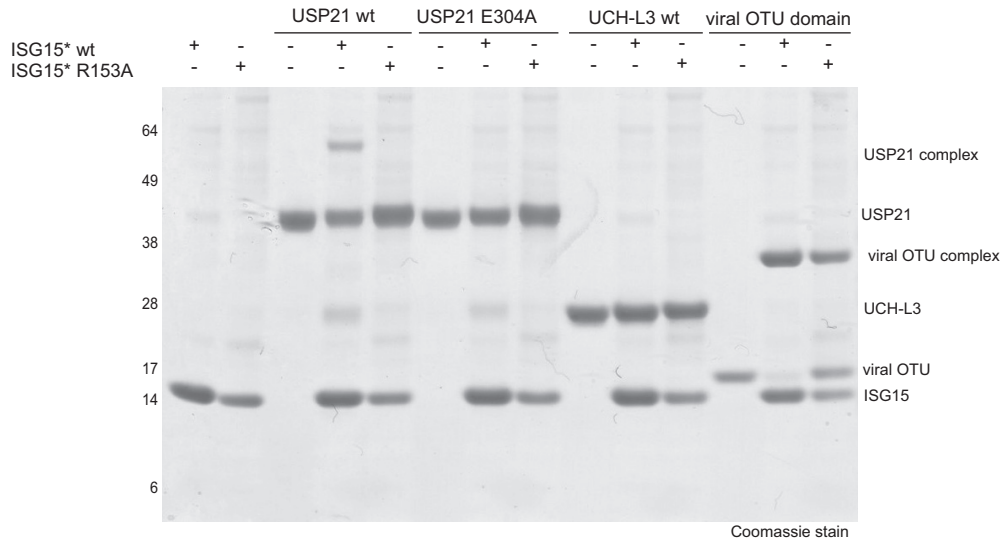
Supplementary Figure 6

USP21 binding to Ub FlAsH

USP21 wt binding monoUb

Supplementary Figure 6: USP21 binding to Ub-FlAsH

MonoUb in which the C-terminal five residues (RLRGG) were replaced with a Trp-FlAsH-sequence (WCCPGCC) does not bind to USP21 in fluorescence anisotropy studies. Error bars represent standard deviation from mean.

Supplementary Figure 7: ISG15 suicide probe assays

ISG15 and mutant ISG15 suicide probes (ISG15-C2Cl, and ISG15R153A-C2Cl) were generated and tested against USP21wt and USP21E304A. Arg153 in ISG15 corresponds to Arg72 in Ub. Only wild-type proteins (i.e. USP21wt and ISG15-C2Cl) resulted in covalent modification, and neither the USP21E304A mutant, nor a mutant probe ISG15R153A-C2Cl), generated a covalent modifier complex. Modification of USP21 with ISG15 suicide probes was not quantitative, suggesting lower reactivity towards this probe, consistent with lower activity of USP21 against ISG15-AMC. UCH-L3 is not modified by ISG15 probes, and hence as a positive control, a recently described viral OTU domain of Crimean Congo hemorrhagic fever virus (CCHFV, (Frias-Staheli et al, 2007)) with cross-reactivity against Ub and ISG15 was utilised. This enzyme was modified quantitatively with ISG15-C2Cl and to a lesser extent with ISG15R153A-C2Cl. All ISG15 probes comprised the stabilising C78S mutation, indicated by ISG15* (Narasimhan et al, 2005).